https://doi.org/10.48048/tis.2024.8195

Effect of Mitochondrial DNA T15663C Mutation on Type 2 Diabetes Mellitus and Cataract Patients, Molecular Dynamics Simulation Study

Fanny Rizki Rahmadanthi[1], Ahmad Fariz Maulana[1], Wanda Destiarani[2], Shabarni Gaffar[1,2] and Iman Permana Maksum[1,*]

[1]Department of Chemistry, Faculty of Mathematics and Natural Sciences, Universitas Padjadjaran, Sumedang, Indonesia
[2]Research Center for Molecular Biotechnology and Bioinformatics, Universitas Padjadjaran, Bandung, Indonesia

([*]Corresponding author's e-mail: iman.permana@unpad.ac.id)

Received: 14 March 2024, Revised: 24 April 2024, Accepted: 19 May 2024, Published: 20 September 2024

Abstract

Diabetes mellitus is a metabolic disease characterized by hyperglycemia. Type 2 diabetes mellitus patients are known to have mutations in their mitochondrial DNA (mtDNA). mtDNA easily undergoes mutations because it does not have histone proteins for protection and lacks a proofreading mechanism during its replication. The mtDNA mutations T15663C found in type 2 diabetes mellitus patients sufferers with a cataract disease. This mutation was found to occur in the cytochrome b gene, one of the gene in the complex III respiratory chain. In this study we investigate the effect of this mutation on the structure of cytochrome b using molecular dynamics simulations using PDB ID: 5XTE as a template and carrying out simulations for 250 ns. The models of wild type and mutant protein structure were constructed using CHARMM-Gui so that, the protein was looked like in the mitochondrial membrane. The results of the molecular dynamics simulation show that the potential energy of the wild type model is lower than the mutant model, the RMSD value of the wild type model is more stable at 114 - 180 ns, and the RMSF value in the wild type model does not fluctuate as much as the mutant model. In addition, the hydrogen bond (H bond) analysis of the mutant model has a higher H bond number than the wild type model, which means that the mutant model is more rigid. The simulation results were visualized using VMD, and new hydrogen bonds were found in the mutant model.

Keywords: T15663C mutation, Molecular dynamics, Cytochrome b, Type 2 diabetes mellitus

Introduction

Mitochondrial DNA has a higher mutation rate, approximately 10 to 17-fold higher than that of chromosomal DNA, primarily due to insufficient DNA repair mechanisms to counteract oxidative damage [1,2]. In addition, mitochondrial DNA lacks histone proteins, rendering it more susceptible to mutation. Mutations that occur in mitochondrial DNA [3]. In July 2018, 349 pathogenic point mutations were reported, and by Novermber 2023 this number increased by 32 % to 461 [3,4].

Mitochondria function as energy producers in the form of adenosine triphosphate (ATP) through oxidative phosphorylation (OXPHOS). ATP is the source of free energy to perform chemical reactions that require energy in the cells, such as protein biosynthesis, cell growth and muscle work [5]. When the

production of ATP in mitochondrial is disrupted which can be caused by mutations of the genes in mtDNA, it will lead to various diseases, such as type 2 diabetes mellitus, cataracts, Leber's hereditary optic neuropathy (LHON), maternally inherited diabetes and deafness (MIDD) mitochondrial encephalomyopathy, lactic acidosis and stroke-like episodes (MELAS), progressive external ophthalmoplegia (PEO), myoclonic epilepsy with ragged-red fibers (MERRF), Kearns-Sayre syndrome (KSS), Alzheimer's disease, Parkinson's disease and cancer [2,6].

DNA mutations have been identified using several methods of damp lab activities, including high-performance liquid chromatography (HPLC), dot-blot hybridization, pyrosequencing, electrochemical biosensors, radio-labeled polymerase chain reaction (PCR), ligation-mediated PCR (LM-PCR), PCR-amplification of specific alleles (PASA), PCR-restriction fragment length polymorphism (PCR-RFLP) and quantitative PCR (qPCR) [6-17]. *In silico* studies related to DNA mutations have also been performed using dynamic molecular simulations, including an understanding of the effect of T10609C and C10676G mutations on proton translocation in ND4-ND4L protein complex I and the effect of dimerization of A3243G mutations on its stability [19,20].

A new point mutation has been discovered in individuals with type 2 diabetes mellitus and cataract phenotypes, one of which was T15663C [20]. This mutation occurs in the cytochrome b gene, a constituent of complex III respiratory chain. Bioinformatics studies have been carried out for this mutation type using Accelrys Discovery Studio, employing PDB ID: IL0L (*Bos taurus*) and PDB ID: 5XTE (*Homo sapiens*) to assess the effect of mutation on protein structure, including the loss of hydrogen bonds and hydrophobic interactions, as well as trajectory analysis. However, molecular dynamics simulations have not been performed previously [4,22]. The molecular dynamics simulations are needed to study the effect of mutations on the stability of protein structure and to determine the relationship between the mtDNA mutation and the cause of the disease. Systems at the molecular level can be simulated using computational chemistry methods or *in silico* methods because this method can reveal the interactions of a system that cannot be simulated by another method [22]. This study uses molecular dynamics simulations to investigate the effects of the mtDNA T15663C mutation on cytochrome b structure.

Materials and methods

Materials

Nucleotide sequence of cytochrome b gene were obtained from the National Center for Biotechnology Information (NCBI) with accession number NC_012920 using Genome Data Viewer. Cytochrome b templates were obtained from MITOMAP. Subsequently, the sequences were aligned using the Basic Local Alignment Search Tool (BLAST) with the PDB (Protein Data Bank) database to acquire templates. The result showed 5XTE as the protein template with the highest homology. The mutant sequences were generated by duplicating wild type data and substituting the amino acid from isoleucine to threonine at position 306.

Methods

Model preparation

The wild type and mutant models of cytochrome b were constructed using Modeller10.4 with 5XTE as a template, generating fifty models for each wild type and mutant. A model with the lowest DOPE (Discrete Optimised Protein Energy) score was chosen as the most reliable and likely to the wild type structure. Subsequently, the model was checked using the Phi (φ) and Psi (ψ) distributions in the Ramachandran Plot generated with the PROCHECK program (https://saves.mbi.ucla.edu/). The presence

of > 90 % residues (amino acids) in the favored region indicated the high quality and stability of the protein model.

The Membrane Builder tool in CHARMM-Gui (https://charmm-gui.org/) was used to construct the phospholipid bilayer system [24,25]. However, the structures in .pdb format could not be read by CHARMM-Gui because they lacked orientation information on membrane proteins. Therefore, it was necessary to superimpose homology results on pre-oriented protein structures from the Orientations of Proteins in Membrane database (OPM) (https://opm.phar.umich.edu/). The lipid used was 1-palmitoyl-2-oleoylphosphatidylcholine (POPC), one of the most prevalent lipids in the inner mitochondrial membrane (IMM) [25]. Additionally, the system was solvated using the transferable intermolecular potential with 3 points (TIP3P) and 150 mM of K^+/Cl^- ions were added to the system to neutralize the amount of charge and ensure a physiologically relevant ionic content [26]. Then, the system was converted into Amber format using the Python charmmlipid2amber.py program in Amber20. Then, the structure from CHARMM-Gui could be read using Load, Energy and Minimize Protein (LEaP) [27].

Molecular dynamics (MD) simulation

Molecular dynamics (MD) simulation was conducted on an Intel Xeon CPU with 16 GiB of memory using Amber20. The protein complex structure was input into the LEaP program. The force fields used are ff14SB, lipid14, gaff2 and tip3p. The system underwent 3 stages of minimization: The minimization of water molecules only, the minimization of proteins and the minimization of the entire system [19,28]. All systems were heated from 0 to 300 K after the minimization process. The system was then equilibrated at constant temperature and pressure to allow for the relaxation of the water molecules. All simulations were performed at constant temperature for 250 ns. The trajectories, including potential energy, Root Mean Square Deviation (RMSD), Root Mean Square Fluctuation (RMSF) and hydrogen bonds (H bonds) obtained from the simulation results were analyzed using Amber20 and visualized with Visual Molecular Dynamics (VMD).

Results and discussion

Cytochrome b is a constituent of complex III in the respiratory chain and plays a crucial role in electron transfer. Cytochrome b comprises 2 components, namely 2 heme groups and iron-sulfur (Fe-S) centers, which capture electrons from ubiquinol (QH_2) and release them to ubiquinone (Q) via heme. The T15663C mutation in cytochrome b can potentially impact its function. To assess the functionality of the wild type and mutant protein, it must exhibit a structural form that appropriate to its physiological conditions, enabling the determination of whether the protein is functioning properly. Therefore, to compare the wild type and mutant models, this study evaluates the potential energy, Root Mean Square Deviation (RMSD), Root Mean Square Fluctuation (RMSF) and hydrogen bonds (H bonds) of the cytochrome b.

In this study, the wild type and mutant models of cytochrome b were constructed using the homology modeling method, employing the wild type cytochrome b sequence obtained from NCBI as the target protein. The cryo-EM structure of human respiratory complex III (cytochrome bc1 complex), with the PDB ID: 5XTE and a resolution of 3.4 Å, was selected as the template model. Utilizing high-resolution reconstruction (< 4 Å) ensures detailed atomic-level models, including both the placement of backbone and sidechain atoms [29]. Homology modeling was implemented with the help of the Modeller10.4 program to generate 3-dimensional structures for both the wild type and mutant cytochrome b proteins. The program was directed to produce 50 models, with a primary assessment based on the DOPE score. Subsequently, the model with the lowest DOPE score was chosen. Specifically, the DOPE score was determined to be -

49,685.57031 for the wild type model and −49,424.15625 for the mutant model.

To validate the structure created as a result of homology modeling, it is necessary to align the template sequence with the mutant. Using Pairwise Sequence Alignment (PSA), the results obtained show an identity and similarity of 99.7 % and the position of the difference mutation point, namely the change in the amino acid isoleucine to threonine at position 306 (**Figure 1**).

```
Length: 378
Identity:     377/378 (99.7%)
Similarity:   377/378 (99.7%)

 1 KTPMRKTNPLMKLINHSFIDLPTPSNISAWWNFGSLLGACLILQITTGLF     50
   |||||||||||||||||||||||||||||||||||||||||||||||||||
 1 KTPMRKTNPLMKLINHSFIDLPTPSNISAWWNFGSLLGACLILQITTGLF     50

51 LAMHYSPDASTAFSSIAHITRDVNYGWIIRYLHANGASMFFICLFLHIGR    100
   |||||||||||||||||||||||||||||||||||||||||||||||||||
51 LAMHYSPDASTAFSSIAHITRDVNYGWIIRYLHANGASMFFICLFLHIGR    100

101 GLYYGSFLYSETWNIGIILLLATMATAFMGYVLPWGQMSFWGATVITNLL    150
    |||||||||||||||||||||||||||||||||||||||||||||||||||
101 GLYYGSFLYSETWNIGIILLLATMATAFMGYVLPWGQMSFWGATVITNLL    150

151 SAIPYIGTDLVQWIWGGYSVDSPTLTRFFTFHFILPFIIAALATLHLLFL    200
    |||||||||||||||||||||||||||||||||||||||||||||||||||
151 SAIPYIGTDLVQWIWGGYSVDSPTLTRFFTFHFILPFIIAALATLHLLFL    200

201 HETGSNNPLGITSHSDKITFHPYYTIKDALGLLLFLLSLMTLTLFSPDLL    250
    |||||||||||||||||||||||||||||||||||||||||||||||||||
201 HETGSNNPLGITSHSDKITFHPYYTIKDALGLLLFLLSLMTLTLFSPDLL    250

251 GDPDNYTLANPLNTPPHIKPEWYFLFAYTILRSVPNKLGGVLALLLSILI    300
    |||||||||||||||||||||||||||||||||||||||||||||||||||
251 GDPDNYTLANPLNTPPHIKPEWYFLFAYTILRSVPNKLGGVLALLLSILI    300

301 LAMIPILHMSKQQSMMFRPLSQSLYWLLAADLLILTWIGGQPVSYPFTII    350
    |||||.|||||||||||||||||||||||||||||||||||||||||||
301 LAMIPTLHMSKQQSMMFRPLSQSLYWLLAADLLILTWIGGQPVSYPFTII    350

351 QVASVLYFTTILILMPTISLIENKMLKW    378
    ||||||||||||||||||||||||||||
351 QVASVLYFTTILILMPTISLIENKMLKW    378
```

Figure 1 Pairwise sequence alignment of the template and mutant cytochrome b. Red box shows the location of differences in mutations in the form of amino acids.

The modeling results are shown in **Figure 2** with differentiation of mutation points based on amino acids. Thus, both models were analyzed using the PROCHECK program, with data extracted from the Ramachandran Plot. In **Figure 3**, the results indicated that both protein models exhibited more than 90 % of their residues in the most favorable region, with only 1 residue in the disallowed region. Specifically, in the wild type model, the residue Ile267 was located in this disallowed region, while in the mutant model, the residue Asn285 occupied a similar position. These residues are situated within loop structures and at the termini of helices, suggesting minimal impact on overall structural stability. Nonetheless, an optimization process was conducted to refine the structural models further. Loop optimization was performed to eliminate residues within regions categorized as disallowed. This optimization procedure was executed using Modeller10.4 and repeated iteratively until all residues were situated within the most favored regions. This ensured the lowest DOPE score, indicative of the model's optimal structure. Following optimization, all residues were found within the most favored regions, 95.1 % for the wild type model and 94.8 % for the mutant model. The plot is shown in **Figure 3**, indicate the models' stereochemical integrity.

The T15663C mutation involves a substitution of thymine (T) to cytosine (C) at position 15,663 corresponding to substitution of isoleucine (Ile) to threonine (Thr) at position 306 in the mitochondrial cytochrome b complex III subunit proteins. Ile is a nonpolar and hydrophobic amino acid, while Thr is polar due to the presence of a hydroxyl group in its side chain. In the wild type model, a hydrogen bond exists between the nitrogen atom of Ile306 and the oxygen atom of Met303, along with a hydrophobic interaction between Ile306 and Met303 (**Figure 4**). The hydrophobic interaction is lost in the mutant model, although hydrogen bond between the nitrogen atom of Thr306 and the oxygen atom of Met303 is retained following the amino acid substitution. Hydrophobic interactions occur between nonpolar molecules, such as Met and Ile, whereas Thr is polar. Consequently, this interaction is present in the wild type model but absent in the mutant model (**Figure 4**). The loss of this interaction adversely affects the stability of the structure, as such interactions play a crucial role in stabilizing protein structures. This observation aligns with previous research, highlight the significance of hydrophobic interactions in maintaining the stability of helical chains [4].

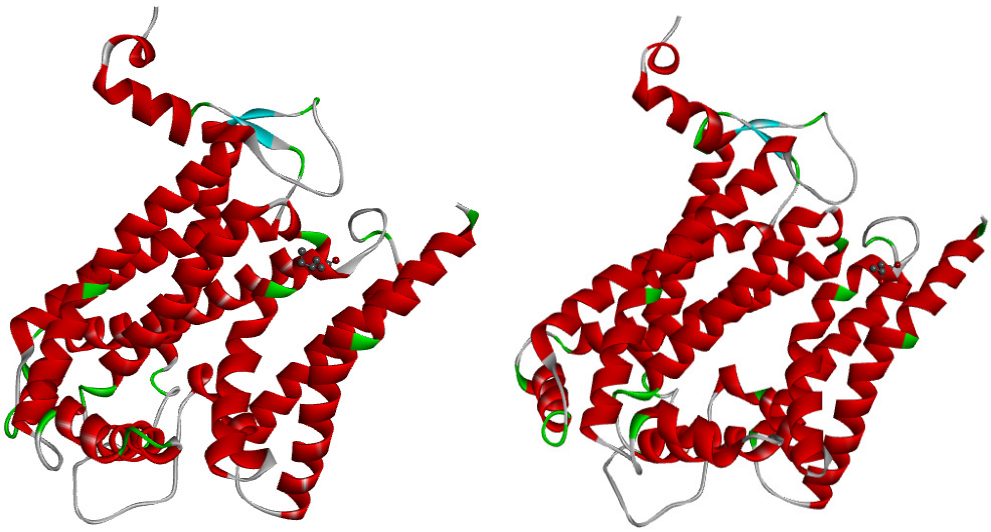

Figure 2 The wild type (left) and mutant (right) model of cytochrome b, were generated using Modeller 10.4 with the lowest DOPE score.

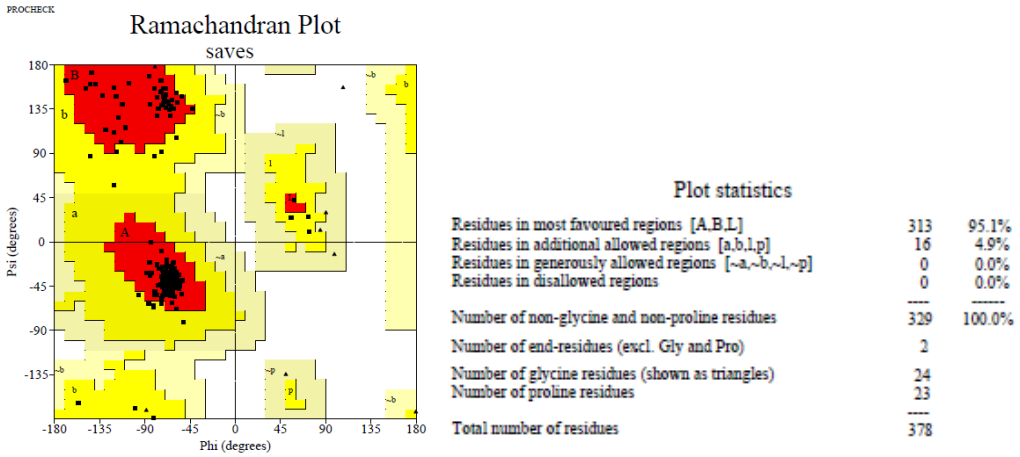

(a)

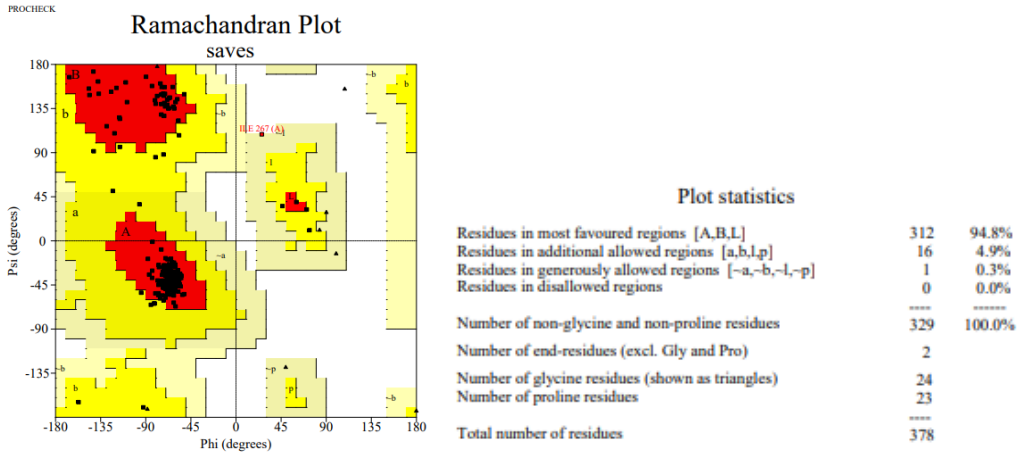

(b)

Figure 3 Ramachandran Plot after loop optimization of wild type (a) and mutant model (b).

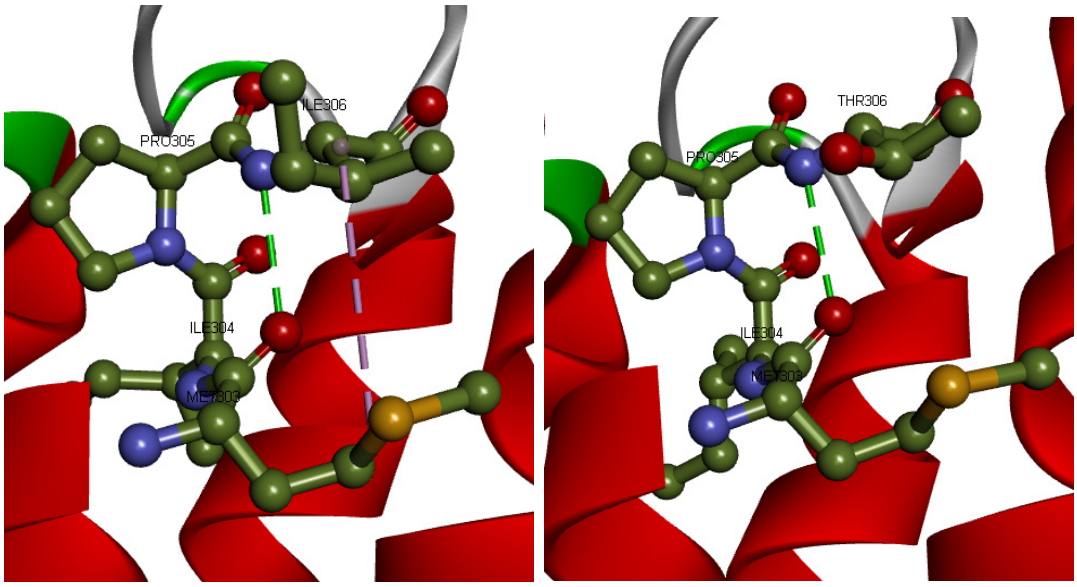

Figure 4 Changes in interactions in the wild type (left) and mutant cytochrome b (right) models. A green dashed line indicates hydrogen bond and hydrophobic interactions are indicated by a purple dashed line.

The structural models were then embedded in a lipid bilayer or mitochondrial membrane using the CHARMM-Gui program, facilitating Molecular Dynamics (MD) simulations. Molecular dynamics simulations enable the analysis of atomic-level motion over time, providing insights into protein behavior and stability [30]. The embedded models were then used analysed the potential energy, Root Mean Square Deviation (RMSD), Root Mean Square Fluctuation (RMSF) and hydrogen bonds (H bonds).

The potential energy can be used to determine the quality and stability of the protein structure, whether it is optimal, suboptimal, or flawed based on its energy value. Optimal structures generally exhibit lower energy values, whereas suboptimal or flawed structures tend to have higher values [31]. In **Figure 5**, the potential energy of the mutant model is higher than that of the wild type model, indicating that the quality of the wild type structure is better.

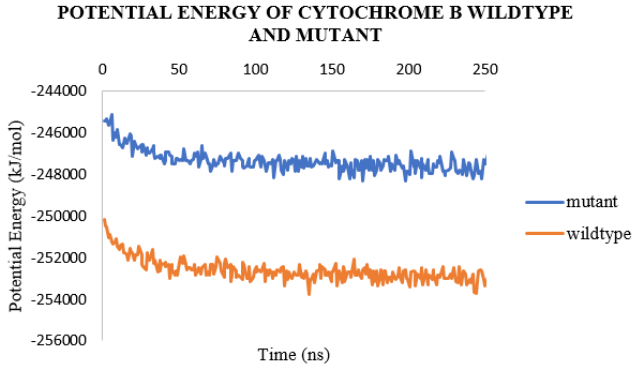

Figure 5 The potential energy of wild type and mutant cytochrome b. Red line: Wild type; blue line: Mutant model. The wild-type model has lower energy than the mutant model.

RMSD is one of the important parameters to measure protein structural stability [32]. RMSD analyzes movements based on time, indicating whether a structure remains stable on a simulated time scale or deviates from its initial coordinates during simulation. RMSDs were calculated for the mutant model and compared with those obtained for the wild type model. The RMSD graph shows all residues of both models in **Figure 6**. Overall, the mutant model exhibits more significant fluctuations than the wild type model. Specifically, during the 114 - 180 ns timeframe, the mutant model fluctuates within the range of 16.73 - 25.22 Å, whereas the wild type model fluctuates within the range of 19.64 - 27.81 Å.

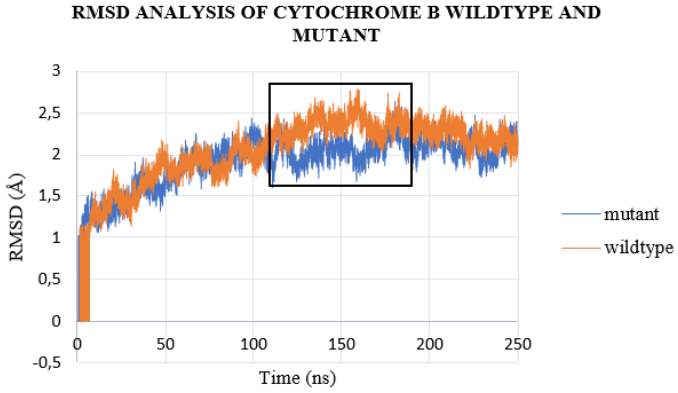

Figure 6 RMSD analysis of wild-type and mutant cytochrome b. Red line: Wild typewild type model; blue line: Mutant model. The mutant model experienced larger fluctuations than a wild type model, specifically during the 114 - 180 ns (shown in the black box).

Furthermore, the RMSF analysis of all residues indicates that fluctuations observed in each residue show the level of flexibility within the structure to determine the stability [33]. RMSF values for mutant backbone residues were calculated and compared with those of the wild type model to determine how the mutation affects the dynamic behavior of residues. Analysis of the fluctuation scores revealed alterations in the flexibility of amino acids in the mutant model. Various high and low peaks, differing from those in the wild type model, were observed in the mutant model, providing evidence that the presence of mutations affects the residue stability. In **Figure 7**, the RMSF values for wild type residues fluctuate within the range of 0.54 - 3.53 Å throughout the entire simulation period. Conversely, the mutant model exhibits fluctuations within the range of 0.59 - 4.06 Å. In addition, the wild type model experienced sharp fluctuations in several areas compared to the mutant model. However, if traced around the residue that experienced the mutation, the mutant model experienced more fluctuations, specifically at residues 243 - 345.

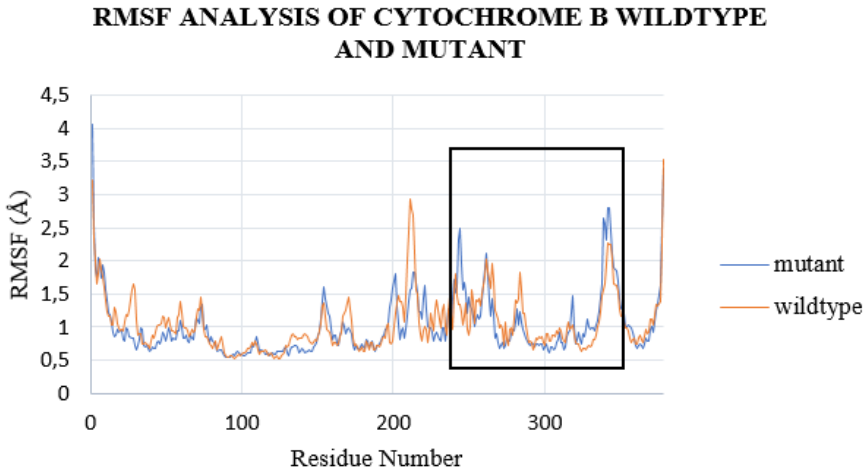

Figure 7 RMSF analysis of cytochrome b. Red line: Wild type model; blue line: Mutant model. At residues 243 - 345, in the mutant model it fluctuates more than in the wild type model (shown in the black box).

Table 1 Acceptor and donor intermolecular hydrogen interactions of wild type and mutant models that occur during simulation.

Model	Acceptor	H Donor	Donor	Frame	Fraction	Simulation time (ns)
Wild type	MET_302@O	ILE_306@H	ILE_306@N	2677	0.1071	26.775
Mutant	MET_302@O	THR_306@H	THR_306@N	13556	0.5422	135.55

To further gain an insight into how mutations at this position affect the interaction between subunits of the protein, analysis of hydrogen bonds (H bonds) is carried out between the nitrogen atom of Ile306 and the oxygen atom of Met303 for wild type model and the nitrogen atom of Thr306 and the oxygen atom of Met303 mutant model. H bonds are one of the components responsible for a protein's secondary and tertiary structure. H bonds help in protein folding and stabilization and play a role in a protein's interaction [34]. A more significant number of H bonds indicates structural rigidity and increased covalent interactions between the 2 subunits. A lower number of H bonds were available to participate in the protein's interaction with the solvent [35].

Interactions above 10 % of the simulation time are considered to be influential in the simulation, which indicates a prolonged involvement [28]. **Table 1** shows the H bonds analysis of mutant model has 54.22 %, which is very high compared with 10.71 % in the wild type model. A slight increase in the number of hydrogen bonds in the mutant model contributes to increased intermolecular interactions and reduced flexibility, and additional movement or any disruption can significantly change the activity of the protein. The reduced space for the protein to move due to the increase in the number of hydrogen bonds in the mutant model compared to the wild type model indicates that the mutant structure is more rigid and challenging for the protein to interact with. The structure of the simulation results was verified to confirm the results of the hydrogen bond analysis. In the mutant model, a new hydrogen bond formed between Thr306 and Met303, whereas it did not occur in the wild type model; it is shown in **Figure 6**. This indicates that there was an increase in hydrogen bonds in the mutant model, as well as a change in structure.

Analysis of hydrogen bonds in mutant models which was higher than wild type models also occurred in research [19], mutations that occurred in mitochondrial DNA were found to affect the protein's function as a proton translocation pathway. Therefore, further research is needed, such as examining the impact of this mutation using *in silico* advanced methods and wet lab research.

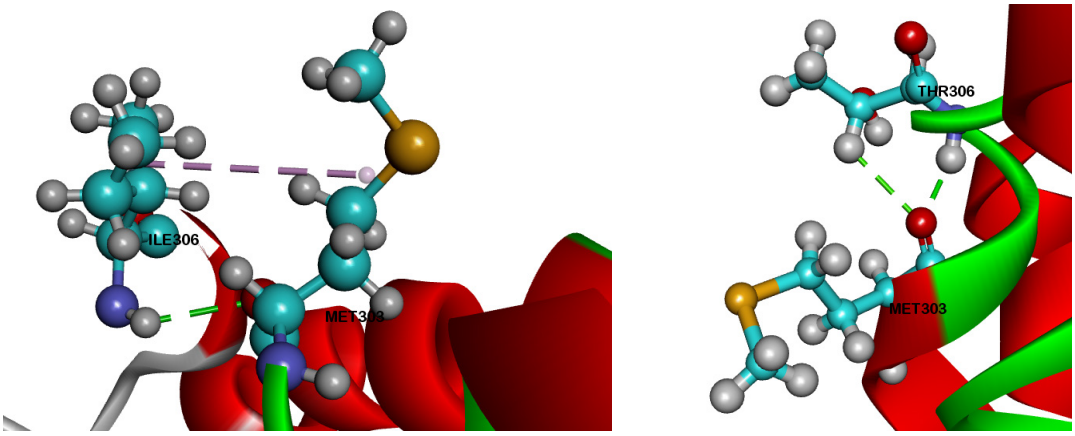

(a) (b)

Figure 8 Interactions in wild type (a) and mutant (b) model after simulations. Hydrogen bonds appear in the mutant model but not in the wild type model, validating the rigidity of the mutant model. A green dashed line indicates hydrogen bonds and hydrophobic interactions are indicated by a purple dashed line.

Conclusions

Mitochondria are one of the body's crucial organelles because they are the site of energy production and will later be sent to other organelles for activities. A mutation is often found in the mitochondria, especially in mitochondrial DNA (mtDNA). Substitution mutation has a significant impact on protein stability. However, protein stability or rigidity can be observed through *in silico* research, one of which is molecular dynamics simulations. This simulation was carried out to determine the differences that exist in the wild type and mutant model, making it possible to decide on the next step regarding whether the mutation will impact the function of the protein.

Four parameters were used in this research are potential energy, Root Mean Square Deviation (RMSD), Root Mean Square Fluctuation (RMSF) and hydrogen bond (H bonds) analysis. The result of simulation show the energy potential of the wild type model is lower than the mutant model and RMSD

values for the wild type model than the mutant model. In addition, the RMSF graph shows that the mutant model tended to fluctuate more than the wild type model. Also, the H bonds analysis showed that the mutant number was higher than the wild type model, indicating that the mutant model was more rigid, making it difficult to interact with other residues or proteins. Further studies are needed to validate the *in silico* results, such as biochemical assays and *in vivo* experiments.

Acknowledgments

This research was funded by Padjadjaran University in the form of Penelitian Dasar Kompetitif Nasional (PDKN), Indonesia Number: 044/E5/PG.02.00.PL/2023 and Number: 1834/UN.6.3.1/PT.00/2023.

References

[1] HAL Tuppen, EL Blakely, DM Turnbull and RW Taylor. Mitochondrial DNA mutations and human disease. *Biochim. Biophys. Acta Bioenerg.* 2010; **1797**, 113-28.

[2] FR Rahmadanthi and IP Maksum. Transfer RNA mutation associated with type 2 diabetes mellitus. *Biology* 2023; **12**, 871.

[3] MITOMAP, Available at: https://www.mitomap.org/MITOMAP, accessed November 2023.

[4] R Mulyani, W Destiarani, UM Rahmawati, M Yusuf, T Subroto and IP Maksum. An investigation of the effect of T15458C and T15663C mutations in the CYB gene on respiration via an *in silico* method. *J. Proteonomics Bioinf.* 2018; **13**, 1-8.

[5] S Casagrande, M Dzialo, L Trost, K Malkoc, ET Sadowska, M Hau, B Pierce, S McWilliams and U Bauchinger. Mitochondrial metabolism in blood more reliably predicts whole-animal energy needs compared to other tissues. *iScience* 2023; **26**, 108321.

[6] C Yan, X Duanmu, L Zeng, B Liu and Z Song. Mitochondrial DNA: Distribution, mutations, and elimination. *Cells* 2019; **8**, 379.

[7] IP Maksum, S Sriwidodo, O Suprijana, G Natadisastra, S Nuswantara and AS Noer. Identifikasi Mutasi Heteroplasmi A3243G DNA Mitokondria dan Studi Pewarisan Maternal pada Pasien Diabetes Melitus Tipe 2 (*in Indonesian*). *Bionatura Jurnal Ilmu-ilmu Hayati dan Fisik* 2010; **12**, 78-85.

[8] AM Ilmi, M Rahmaniar and MI Permana. Design and optimization of PCR-RFLP assay for detection of G9053A and T15663C mutation in mitochondrial DNA. *Res. J. Chem. Environ.* 2023; **27**, 1-5.

[9] A Biggin, R Henke, B Bennetts, DR Thorburn and J Christodoulou. Mutation screening of the mitochondrial genome using denaturing high-performance liquid chromatography. *Mol. Genet. Metabol.* 2005; **84**, 61-74.

[10] ML Smith, XY Hua, DL Marsden, D Liu, NG Kennaway, KY Ngo and RH Haas. Diabetes and mitochondrial encephalomyopathy with lactic acidosis and stroke-like episodes (MELAS): Radiolabeled polymerase chain reaction is necessary for accurate detection of low percentages of mutation. *J. Clin. Endocrinol. Metabol.* 1997; **82**, 2826-31.

[11] HE White, VJ Durston, A Seller, C Fratter, JF Harvey and NCP Cross. Accurate detection and quantitation of heteroplasmic mitochondrial point mutations by pyrosequencing. *Genet. Test.* 2005; **9**, 190-9.

[12] M Urata, M Wakiyama, M Iwase, M Yoneda, S Kinoshita, N Hamasaki and D Kang. New sensitive method for the detection of the A3243G mutation of human mitochondrial deoxyribonucleic acid in diabetes mellitus patients by ligation-mediated polymerase chain reaction. *Clin. Chem.* 1998; **44**, 2088-93.

[13] YW Hartati, SN Topkaya, IP Maksum and M Ozsoz. Sensitive detection of mitochondrial DNA A3243G tRNALeu mutation via an electrochemical biosensor using meldola's blue as a hybridization indicator. *Adv. Anal. Chem.* 2013; **3**, 20-7.

[14] RAI Chandra, S Sriwidodo, A Diantini and IP Maksum. Restriction enzymes apai analysis to find A3243G mutation in indonesia diabetes mellitus type II patients. *J. Med. Bioeng.* 2015; **4**, 492-6.

[15] S Sriwidodo, O Suprijana, T Subroto and IP Maksum. Studi mutasi titik A3243G DNA mitokondria penyebab maternally (*in Indonesian*). *Majalah Ilmu Kefarmasian* 2008; **3**, 121-9.

[16] IP Maksum, A Farhani, SD Rachman and Y Ngili. Making of the A3243G mutant template through site directed mutagenesis as positive control in PASA-Mismatch three bases. *Int. J. Pharmtech Res.* 2013; **5**, 441-50.

[17] E Rong, H Wang, S Hao, Y Fu, Y Ma and T Wang. Heteroplasmy detection of mitochondrial DNA A3243G mutation using quantitative real-time PCR assay based on TaqMan-MGB probes. *Biomed. Res. Int.* 2018; **2018**, 1286480.

[18] IP Maksum, AF Maulana, M Yusuf, R Mulyani, W Destiarani and R Rustaman. Molecular dynamics simulation of a tRNA-leucine dimer with an A3243G heteroplasmy mutation in human mitochondria using a secondary structure prediction approach. *Ind. J. Chem.* 2022; **22**, 1043-51.

[19] W Destiarani, R Mulyani, M Yusuf and IP Maksum. Molecular dynamics simulation of T10609C and C10676G mutations of mitochondrial *ND4L* gene associated with proton translocation in type 2 diabetes mellitus and cataract patients. *Bioinf. Biol. Insights* 2020; **14**, 1-8.

[20] IP Maksum, R Mulyani, K Hasan, MI Azizah, W Destiarani, AF Maulana, M Yusuf and T Subroto. Study on the mitochondrial genome of variants carrying mt.3243A>G from type-2 diabetes mellitus and cataract patients in Indonesia. *Hayati* 2023; **30**, 1017-24.

[21] IP Maksum, S Safitri, M Yusuf, SN Nuswantara and O Suprijana. Structure and function of CYB in type-2 diabetes mellitus and cataract patients which associated with mitochondrial DNA mutation. *In*: Proceeding of the 1st International Conference on Computation for Science and Technology, Chiang Mai, Thailand. 2010, p. 103-10.

[22] HI Ingólfsson, C Arnarez, X Periole and SJ Marrink. Computational 'microscopy' of cellular membranes. *J. Cell Sci.* 2016; **129**, 257-68.

[23] EL Wu, WX Cheng, S Jo, H Rui, KC Song, EM Davilia-Contreras, Y Qi, J Lee, V Monje-Galvan, RM Venable, JB Klauda and W Im. CHARMM-GUI membrane builder toward realistic biological membrane simulations. *J. Comput. Chem.* 2014; **35**, 1997-2004.

[24] S Jo, T Kim, VG Iyer and W Im. CHARMM-GUI: A web-based graphical user interface for CHARMM. *J. Comput. Chem.* 2008; **29**, 1859-65.

[25] EM Mejia and GM Hatch. Mitochondrial phospholipids: Role in mitochondrial function. *J. Bioenerg. Biomembr.* 2016; **48**, 99-112.

[26] M Kondrashova, M Zakharchenko and N Khunderyakova. Preservation of the *in vivo* state of mitochondrial network for *ex vivo* physiological study of mitochondria. *Int. J. Biochem. Cell Biol.* 2009; **41**, 2036-50.

[27] X Meng, H Liu, N Zhao, Y Yang, K Zhao and Y Dai. Molecular dynamics study of the effect of charge and glycosyl on superoxide anion distribution near lipid membrane. *Int. J. Mol. Sci.* 2023; **24**, 10926.

[28] AF Maulana, IP Maksum, S Sriwidodo and Y Rukayadi. Proposed molecular mechanism of non-competitive inhibition using molecular dynamics simulations between α-glucosidase enzyme and mangostin compound as antidiabetic. *J. Mol. Model.* 2024; **30**, 136.

[29] G Pintilie, DH Chen, CA Haase-Pettingell, JA King and W Chiu. Resolution and probabilistic models of components in CryoEM maps of mature P22 bacteriophage. *Biophys. J.* 2016; **110**, 827-39.

[30] RN Beni, P Elyasi-Ebli, S Gharaghani and A Seyedarabi. *In silico* studies of anti-oxidative and hot temperament-based phytochemicals as natural inhibitors of SARS-CoV-2 M^{pro}. *PLoS One* 2023; **18**, e0295014.

[31] ASMJ Islam, MdS Akbar, MdS Islam, C Stampfl, AG Bhuiyan and J Park. Atomistic details of grain, crack, and notch effect on the mechanical behavior and fracture mechanisms of monolayer silicon carbide. *Mater. Chem. Phys.* 2024; **316**, 129068.

[32] X Zhang, Y Zhang, T Fan, Z Feng and L Yang. Structure-guided engineered urethanase from *Candida parapsilosis* with pH and ethanol tolerance to efficiently degrade ethyl carbamate in Chinese rice wine. *Ecotoxicol. Environ. Saf.* 2024; **276**, 116335.

[33] J Sharma, VK Bhardwaj, R Singh, V Rajendran, R Purohit and S Kumar. An *in-silico* evaluation of different bioactive molecules of tea for their inhibition potency against non-structural protein-15 of SARS-CoV-2. *Food Chem.* 2021; **346**, 128933.

[34] K Kavitha and A Mohanapriya. Insights into the structure–function relationship of missense mutations in the human TOP2A protein in ovarian cancer. *Front. Phys.* 2024; **12**, 01-17.

[35] M Shojapour, F Fatemi, S Farahmand and MD Shasaltaneh. Investigation of Cyc_1 protein structure stability after H53I mutation using computational approaches to improve redox potential. *J. Mol. Graph. Model.* 2021; **105**, 107864.